Inorg. Chem. **2006**, *45*, 5576–5584

Synthesis of the Novel $[W_3PdS_4H_3(dmpe)_3(CO)]^+$ Cubane Cluster and Kinetic Studies on the Substitution of Coordinated Hydrides in Acidic Media

Andrés G. Algarra,[†] Manuel G. Basallote,*[,†] Marta Feliz,[‡] M. Jesús Fernández-Trujillo,[†] Eva Guillamón,[‡] Rosa Llusar,*[,‡] and Cristian Vicent[‡]

Departamento de Ciencia de los Materiales e Ingeniería Metalúrgica y Química Inorgánica, Facultad de Ciencias, Universidad de Cádiz, Apartado 40, Puerto Real, 11510 Cádiz, Spain, and Departament de Ciències Experimentals, Universitat Jaume I, Campus de Riu Sec, Box 224, 12071 Castelló, Spain

Received December 23, 2005

Reaction of the incomplete cuboidal $[W_3S_4H_3(dmpe)_3]^+$ cluster with a Pd(0) complex under a CO atmosphere produces a rare example of a heterodimetallic hydrido cluster of formula $[W_3PdS_4H_3(dmpe)_3(CO)]^+$ ($[\mathbf{1}]^+$). There are not significant changes in the W–W bond lengths on going from the trinuclear to the tetranuclear cluster. The average W–W and W–Pd bond distances of 2.769[10] and 2.90[2] Å, respectively, are consistent with the presence of single bonds between metal atoms. The heterodimetallic $[\mathbf{1}]^+$ complex is easier to oxidize and more difficult to reduce than its trinuclear precursor, which reflects the electron-donating capability of the Pd(CO) fragment. However, mechanistic studies on the reaction of $[\mathbf{1}]^+$ with acids show a lower basicity for this complex in comparison with that of its trinuclear precursor, so there is a major electron-density rearrangement within the cluster core upon Pd(CO) coordination. This rearrangement is also reflected in an unusual expansion of the sulfur tetrahedron within the W_3PdS_4 core with the concomitant elongation of the W–S bond distances by 0.04 Å with respect to the analogous bond lengths in the trinuclear precursor. For those thermodynamically favored proton-transfer processes, the reaction mechanism of $[\mathbf{1}]^+$ with acids is quite similar to that observed for the incomplete trinuclear cluster, with only small changes in the rate constants. The reaction of $[\mathbf{1}]^+$ with HCl in acetonitrile/water mixtures produces $[W_3PdS_4Cl_3(dmpe)_3(CO)]^+$ ($[\mathbf{2}]^+$) in two kinetically distinguishable steps. Proton transfer occurs in the initial step, in which the W–H bonds are attacked by the acid to yield dihydrogen-bonded adducts that are further attacked by an acetonitrile molecule to give $[W_3PdS_4(CH_3CN)_3(dmpe)_3(CO)]^{4+}$ and dihydrogen. The nature of processes involved in the second step are not well-understood with the present data, although it is very likely that these correspond to some secondary processes. In the third resolved step, the coordinated CH_3CN ligands in $[W_3PdS_4(CH_3CN)_3(dmpe)_3(CO)]^{4+}$ are substituted by Cl^- to afford the final $[\mathbf{2}]^+$ product. No reaction is observed between $[\mathbf{1}]^+$ and HCl in neat acetonitrile, whereas the product of the reaction of $[\mathbf{1}]^+$ with HBF_4 or Hpts ($pts^- = p$-toluenesulfonate) in this solvent is $[W_3PdS_4(CH_3CN)_3(dmpe)_3(CO)]^{4+}$. The reaction occurs in a single kinetic step with a first- (Hpts) or second-order (HBF_4) dependence with respect to the acid. The first- and second-order acid dependences can be interpreted through the initial formation of dihydrogen adducts with one or two acid molecules, respectively.

Introduction

Heterodimetallic sulfide clusters of molybdenum and tungsten are nowadays easily accessible through building block strategies starting from incomplete cuboidal $M_3(\mu_3\text{-}S)(\mu\text{-}S)_3$ (M= Mo, W) clusters.[1−5] Cubane type metal sulfide

* To whom correspondence should be addressed. Fax: 34 964 728066 (R.L.). Tel: 34 964 728086 (R.L.). E-mail: llusar@exp.uji.es (R.L); manuel.basallote@uca.es (M.G.B.).

[†] Universidad de Cádiz.

[‡] Universitat Jaume I.

(1) Shibahara, T.; Yamamoto, T.; Sakane, G. *Chem. Lett.* **1994**, 1231.
(2) Hidai, M.; Kuwata, S.; Mizobe, Y. *Acc. Chem. Res.* **2000**, *33*, 46.
(3) Hernandez-Molina, R.; Sokolov, M. N.; Sykes, A. G. *Acc. Chem. Res.* **2001**, *34*, 223.
(4) Sakane, G.; Shibahara, T. *Inorg. Synth.* **2002**, *33*, 150.
(5) Akashi, H.; Isobe, K.; Shibahara, T. *Inorg. Chem.* **2005**, *44*, 3494.

10.1021/ic052184u CCC: $33.50
Published on Web 06/10/2006

complexes have been extensively used as models for the active sites of metalloenzymes and industrial metal sulfide catalysts.[6] Incorporation of palladium into the $M_3(\mu_3\text{-}S)(\mu\text{-}S)_3$ unit has allowed for the preparation of tetrametallic M_3PdS_4 complexes, which exhibit a remarkable catalytic activity for the addition of alcohols and carboxylic acids to electron-deficient alkynes.[7−9] The interest of transition-metal hydrides in catalysis combined with the catalytic activity of these M_3PdS_4 cubane complexes has encouraged us to study the incorporation of Pd into W_3S_4 cluster hydrides.

Trinuclear hydride clusters of group six metals have been isolated only for tungsten within the complex series of formula $[W_3Q_4H_3(\text{diphosphine})_3]^+$ (Q = S, Se; diphos = dmpe, dppe).[10,11] The hydride ligands in these compounds occupy terminal positions, in contrast with the most-common edge-bridging coordination mode found in other trinuclear cluster chalcogenides.[12,13] Up to date, there is only one example of heterodimetallic cubane type sulfido clusters containing hydride ligands, namely the $[Mo_3RuS_4Cp^*_3H_2(PPh_3)]^+$ cation, in which the ruthenium is coordinated to two hydrides and one phosphine.[14] The ruthenium atom in this cluster is quite unique, binding hydrogen reversibly under mild conditions. In addition, this Mo_3RuS_4 hydride cluster is effective for the N−N bond cleavage of hydrazines to produce ammonia and nitrogen.[15]

In this work, we report the synthesis, structure, and electrochemical properties of the $[W_3PdS_4H_3(dmpe)_3(CO)]^+$ ($[\mathbf{1}]^+$) hydrido cubane. This complex is the second example of a cubane type sulfido cluster containing hydride ligands. However, in contrast with the $[Mo_3RuS_4Cp^*_3H_2(PPh_3)]^+$ complex, in which the heterometal bears both hydride ligands, each hydride ligand in $[W_3PdS_4H_3(dmpe)_3(CO)]^+$ occupies a terminal position on each tungsten atom, as found in its trinuclear $[W_3S_4H_3(dmpe)_3]^+$ precursor. The properties of this last trinuclear cluster, air stability and solubility in a wide variety of solvents, make it an excellent substrate for investigating the mechanism of protonation of hydride complexes. Thus, the terminal hydrides in $[W_3Q_4H_3(dmpe)_3]^+$ undergo acid-promoted substitution reactions through the formation of dihydrogen-bonded adducts, with the kinetics and mechanism showing a strong dependence on the coordinating capability of the solvent.[16−18] The tetranuclear cluster shares properties regarding stability and solubility with its trinuclear precursor; as a result of that, it provides a unique opportunity for studying the effect that the incorporation of a second metal has on the basicity and protonation mechanism of the tungsten-coordinated hydrides in these W_3PdS_4 cubane type clusters.

Experimental Section

General Remarks. $[W_3S_4H_3(dmpe)_3][PF_6]$ was prepared according to literature methods.[10] $[Pd_2(dba)_3]$ (dba = dibenzylideneacetone) was purchased from Strem Chemicals. Solvents for synthesis and electrochemical measurements were dried and degassed by standard methods before use.

Physical Measurements. Elemental analyses were performed on an EA 1108 CHNS microanalyzer at the Universidad de La Laguna. $^{31}P\{^1H\}$ NMR spectra were recorded on a Varian MERCURY 300 MHz instrument and were referenced to external 85% H_3PO_4. ^1H, $^{13}C\{^1H\}$, and $^1H-^{13}C$ gHSQC spectra were recorded on a Varian INOVA 500 MHz instrument using CD_2Cl_2 or acetone-d_6 as solvent. Chemical shifts are reported in parts per million from tetramethylsilane with the solvent resonance as the internal standard. IR spectra were recorded on a Perkin−Elmer System 2000 FT-IR instrument using KBr pellets. Signal intensities are denoted as s = strong, m = medium, and w = weak. Electronic absorption spectra were obtained on a Perkin−Elmer Lambda-19 spectrophotometer in dichloromethane. Electrospray mass spectra were recorded with a Quattro LC (quadrupole−hexapole−quadrupole) mass spectrometer with an orthogonal Z-spray electrospray interface (Micromass, Manchester, U.K.). The cone voltage was set at 20 V unless otherwise stated, using CH_3CN as the mobile-phase solvent. Nitrogen was employed as the drying and nebulizing gas. Isotope experimental patterns were compared with theoretical patterns obtained using the MassLynx 4.0 program.[19] Cyclic voltammetry experiments were performed with an Echochemie Pgstat 20 electrochemical analyzer. All measurements were carried out at room temperature with a conventional three-electrode configuration consisting of platinum working and auxiliary electrodes and an Ag/AgCl reference electrode containing aqueous 3 M KCl. Dichloromethane was used as the solvent in all experiments. The supporting electrolyte was 0.1 mol dm^{-3} tetrabutylammonium hexafluorophosphate. $E_{1/2}$ values were determined as being $^1/_2(E_a + E_c)$, where E_a and E_c are the anodic and cathodic peak potentials, respectively. All potentials reported are not corrected for the junction potential. Potentials reported versus SCE have been referenced to Ag/AgCl as $E_{1/2}(\text{SCE}) - E_{1/2}(\text{Ag/AgCl}) = 0.04$ V on the basis of the values provided for the Fc^+/Fc couple.

Synthesis. $[W_3PdS_4H_3(dmpe)_3(CO)][PF_6]$ ($[\mathbf{1}][PF_6]$). To a pink solution of $[W_3S_4H_3(dmpe)_3][PF_6]$ (0.2 g, 0.16 mmol) in CH_2Cl_2 (30 cm^3) was added an excess of $[Pd_2(dba)_3]$ (0.080 g, 0.09 mmol) under nitrogen, and the color changed to red. After CO was bubbled through the solution for 30 min at room temperature, the reaction mixture was stirred for a day under a CO atmosphere and filtered. The resulting solution was then precipitated with Et_2O, and the solid recrystallized from CH_2Cl_2/Et_2O mixtures to afford a red micro-

(6) Brorson, M.; King, J. D.; Kiriakidou, K.; Prestopino, F.; Nordlander, E. In *Metal Clusters in Chemistry*; Braustein, P., Oro, L. A., Raithby, P. R., Eds.; Wiley-VCH: Weinheim, 1999; Vol. 2.
(7) Murata, T.; Mizobe, Y.; Gao, H.; Ishii, Y.; Wakabayashi, T.; Nakano, F.; Tanase, T.; Yano, S.; Hidai, M.; Echizen, I.; Nanikawa, H.; Motomura, S. *J. Am. Chem. Soc.* **1994**, *116*, 3389.
(8) Wakabayashi, T.; Ishii, Y.; Murata, T.; Mizobe, Y.; Hidai, M. *Tetrahedron Lett.* **1995**, *36*, 5585.
(9) Wakabayaskhi, T.; Ishii, Y.; Ishikawa, K.; Hidai, M. *Angew. Chem., Int. Ed.* **1996**, *35*, 2123.
(10) Cotton, F. A.; Llusar, R.; Eagle, C. T. *J. Am. Chem. Soc.* **1989**, *111*, 4332.
(11) Estevan, F.; Feliz, M.; Llusar, R.; Mata, J. A.; Uriel, S. *Polyhedron* **2001**, *20*, 527.
(12) Bright, T. A.; Jones, R. A.; Koschmieder, S. U.; Nunn, C. N. *Inorg. Chem.* **1988**, *27*, 3819.
(13) Kuwata, S.; Andou, M.; Hashizume, K.; Mizobe, Y.; Hidai, M. *Organometallics* **1998**, *17*, 3429.
(14) Takei, I.; Suzuki, K.; Enta, Y.; Dohki, K.; Suzuki, T.; Mizobe, Y.; Hidai, M. *Organometallics* **2003**, *22*, 1790.
(15) Takei, L.; Dohki, K.; Kobayashi, K.; Suzuki, T.; Hidai, M. *Inorg. Chem.* **2005**, *44*, 3768.
(16) Basallote, M. G.; Estevan, F.; Feliz, M.; Fernandez-Trujillo, M. J.; Hoyos, D. A.; Llusar, R.; Uriel, S.; Vicent, C. *Dalton Trans.* **2004**, 530.
(17) Basallote, M. G.; Feliz, M.; Fernandez-Trujillo, M. J.; Llusar, R.; Safont, V. S.; Uriel, S. *Chem.−Eur. J.* **2004**, *10*, 1463.
(18) Algarra, A. G.; Basallote, M. G.; Feliz, M.; Fernandez-Trujillo, M. J.; Llusar, R.; Safont, V. S. *Chem.−Eur. J.* **2006**, *12*, 1413.
(19) *MASSLYNX*, 4.0 ed.; Micromass Ltd.: Manchester, U.K., 2005.

crystalline product characterized as $[W_3PdS_4H_3(dmpe)_3(CO)][PF_6]$ ($[\mathbf{1}][PF_6]$) (0.199 g, 90%). Calcd for $C_{19}H_{51}F_6OP_7PdS_4W_3$: S, 9.08; C, 16.15; H, 3.64. Found: S, 9.02; C, 16.54; H, 3.88. λ_{max} (nm): 515 (sh), 463, 392. IR (cm^{-1}): 2008 (s, CO), 1741 (s, W−H), 1418 (s), 1299 (m), 1285 (m), 1135 (m), 938 (i), 898 (m), 837 (s, P−F), 744 (m), 714 (m), 654 (m), 557 (s, P−F), 423 (w), 338 (w). $^{31}P\{^1H\}$ NMR: δ −143.44 (sept, ^1J(P−F) = 704.0 Hz), −10.12 (d, ^2J(P−P) = 9.7 Hz, ^1J(P−W) = 133.7 Hz), 3.01 (d, ^2J(P−P) = 9.7 Hz, ^1J(P−W) = 181.0 Hz). ^1H NMR: δ −2.68 (3H hydride, dd, ^2J(P−H) = 46.0 Hz, ^2J(P′−H) = 28.5 Hz), 0.86 (9H, C*H*$_3$, d, ^2J(P−H) = 9.0 Hz), 1.51 (3H, C*H*$_2$, m), 1.81 (9H, C*H*$_3$, d, ^2J(P−H) = 8.0 Hz), 1.84 (3H, C*H*$_2$, m), 1.85 (9H, C*H*$_3$, d, ^2J(P−H) = 7.5 Hz), 1.99 (9H, C*H*$_3$, d, ^2J(P−H) = 9.0 Hz), 2.01 (3H, C*H*$_2$, m), 2.40 (3H, C*H*$_2$, m,). $^{13}C\{^1H\}$ NMR: δ 14.71 (CH$_3$, d, ^1J(C−P) = 25.3 Hz), 19.06 (CH$_3$, d, ^1J(C−P) = 24.5 Hz), 21.19 (CH$_3$, d, ^1J(C−P) = 30.2 Hz), 22.54 (CH$_3$, d, ^1J(C−P) = 29.3 Hz), 28.50 (CH$_2$, dd, ^1J(C−P) = 21.8 Hz, ^2J(C−P) = 3.0 Hz), 29.40 (CH$_2$, dd, ^1J(C−P) = 25.7 Hz, ^2J(C−P) = 4.0 Hz). Electrospray-MS (cone voltage 65 V): *m*/*z* 1268 (M^+), 1240 (M^+ − CO).

$[W_3PdS_4Cl_3(dmpe)_3(CO)][PF_6]$ ($[\mathbf{2}][PF_6]$). To a red solution of $[W_3PdS_4H_3(dmpe)_3(CO)][PF_6]$ ($[\mathbf{1}][PF_6]$) (0.07 g, 0.05 mmol) in 5 cm^3 of CH_3CN was added aqueous HCl (3 cm^3, 0.1 M), and the resulting mixture was stirred for 10 min. Partial evaporation of the solvent (ca. 4 cm^3) precipitates the desired product as a red-brown microcrystalline solid, which was filtered; washed with water, 2-propanol, and diethyl ether; and dried to afford $[W_3PdS_4Cl_3(dmpe)_3(CO)][PF_6]$ ($[\mathbf{2}][PF_6]$) (0.065 g, 87%). Calcd for $C_{19}H_{48}Cl_3F_6OP_7PdS_4W_3$: S, 8.45; C, 15.05; H, 3.20. Found: S, 8.41; C, 15.04; H, 3.18. λ_{max} (nm): 549, 413 (sh), 385. IR (cm^{-1}): 2043 (s, CO), 1741 (s, W−H), 1416 (s), 1302 (m), 1286 (m), 1136 (m), 951 (s), 940 (s), 899 (m), 832 (s, P−F), 747 (m), 710 (m), 650 (m), 557 (s, P−F), 438 (w), 415 (w), 336 (w). $^{31}P\{^1H\}$ NMR: δ −143.44 (sept, ^1J(P−F) = 704.0 Hz), −0.50 (s, ^1J(P−W) = 184.4 Hz), −4.12 (s, ^1J(P−W) = 173.5 Hz); ^1H NMR: δ 1.26 (9H, C*H*$_3$, d, ^2J(P−H) = 9.5 Hz), 1.72 (9H, C*H*$_3$, ^2J(P−H) = 9.5 Hz), 1.76 (9H, C*H*$_3$, d, ^2J(P−H) = 11.0 Hz), 1.81 (3H, C*H*$_2$, m), 1.95 (3H, C*H*$_2$, m), 2.01 (9H, C*H*$_3$, ^2J(P−H) = 10.0 Hz), 2.21 (3H, C*H*$_2$, m), 2.55 (3H, C*H*$_2$, m). $^{13}C\{^1H\}$ NMR: δ 12.27 (*C*H$_3$, d, ^1J(C−P) = 29.0 Hz), 12.88 (*C*H$_3$, d, ^1J(C−P) = 26.7 Hz), 14.61 (*C*H$_3$, d, ^1J(C−P) = 32.8 Hz), 19.99 (*C*H$_3$, d, ^1J(C−P) = 31.3 Hz), 27.40 (*C*H$_2$, dd, ^1J(C−P) = 27.5 Hz, ^2J(C−P) = 8.9 Hz), 28.13 (*C*H$_2$, dd, ^1J(C−P) = 23.4 Hz, ^2J(C−P) = 9.1 Hz). Electrospray-MS (cone voltage 65 V): *m*/*z* 1370 (M^+), 1342 (M^+ − CO).

Kinetic Experiments. The kinetics of the reaction of the $[\mathbf{1}]^+$ cluster with acids was studied at 25.0 °C using an Applied Photophysics SX17MV stopped-flow instrument provided with a PDA1 diode-array detector, and the results were analyzed with the SPECFIT program.[20] The experiments were carried out using either CH_3CN-H_2O (1:1 v/v) or neat CH_3CN as solvent. Because solutions of $[\mathbf{1}][PF_6]$ in CH_3CN-H_2O are not stable, the kinetic experiments in this mixture of solvents were carried out by mixing in the stopped-flow instrument solutions of this compound in neat CH_3CN with aqueous solutions of the acid. Although this led to an increase in the dead time for the kinetic experiments in CH_3CN-H_2O mixtures, it did not affect the results; this is because no reaction occurs to a significant extent during the mixing time, so the data could be always fitted satisfactorily using the appropriate model (single or consecutive exponentials) and yielded reproducible values of the rate constants. The solutions of acid contained in all cases the amount of Et_4NBF_4 or Li(pts) required to achieve a constant ionic strength of 0.1 mol dm^{-3} in the solution arriving in the stopped-flow cell. The concentration of acid was determined in each case by titration with a previously standardized KOH solution; for the acid solutions in CH_3CN, the titrations were carried out after diluting an aliquot (1−2 cm^3) with water (50 cm^3). For the kinetic experiments in neat CH_3CN, HCl was generated by reaction of $ClSiMe_3$ with MeOH.

X-ray Studies. Replacement of the PF_6^- anion in cluster $[\mathbf{1}][PF_6]$ was done by adding an excess of $Na[BPh_4]$ to a methanol solution of $[\mathbf{1}]^+$ that precipitates the desired tetraphenylborate salt. Suitable crystals for X-ray studies for compound $[\mathbf{1}][BPh_4]$ were grown by slow diffusion of toluene into a sample solution in CH_2Cl_2. The crystals are air-stable and were mounted on the tip of a glass fiber with the use of epoxy cement. X-ray diffraction experiments were carried out on a Bruker SMART CCD diffractometer using Mo−Kα radiation (λ = 0.71073 Å) at room temperature. The data were collected with a frame width of 0.3° in ω and a counting time of 10 s per frame. The diffraction frames were integrated using the SAINT package and corrected for absorption with SADABS.[21,22] The structures were solved by direct methods and refined by the full-matrix method on the basis of F^2 using the SHELXTL software package.[23] The structure of $[\mathbf{1}][BPh_4]$ was successfully solved in the monoclinic *C*2/*c* space group. All non-hydrogen atoms both in the cluster and the tetraphenylborate anion were refined anisotropically. The positions of all hydrogen atoms were generated geometrically, assigned isotropic thermal parameters, and allowed to ride on their respective parent carbon atoms. Crystal data for $[\mathbf{1}][BPh_4]$: $BC_{43}H_{71}F_6OP_6PdS_4W_3$, M = 1586.82, monoclinic, space group *C*2/*c*, a = 32.037(3) Å, b = 21.782(2) Å, c = 22.351(2) Å, β = 134.204(2)°, V = 11181.1(18) Å^3, T = 293 K, Z = 8, ρ_{calcd} = 1.885 g/cm^3, μ(MoKα) = 6.820 mm^{-1}. Number of reflections collected/unique = 38 487/12 821 (R_{int} = 0.0928). Final refinement converged with R_1 = 0.0489 for 7305 reflections with $F_0 \geq 4\sigma(F_0)$ and wR_2 = 0.1162 for all reflections, GOF = 1.028, max/min residual electron density 1.624/−1.384 e Å^{-3}.

Results and Discussion

Synthesis and Redox Properties. Trinuclear $M_3(\mu_3\text{-}S)(\mu\text{-}S)_3$ (M = Mo, W) cubane type clusters have been widely used as metalloligands toward other transition metals to produce a large variety of heterodimetallic $M_3M'(\mu_3\text{-}S)_4$ complexes.[24] This chemistry has been mainly developed in water; the major advances are found for molybdenum clusters, for which the heterometals incorporated range from group 6 to group 15 elements.[25,26] For tungsten, the number of heterometals is more restricted, namely In, Ge, Sn, Mo, Re, Ni, Pt, and Cu; this fact has been attributed to the greater difficulty in reducing tungsten compared to molybdenum. The formation of the $[M_3PdS_4]^{n+}$ aquo ion has only been shown for molybdenum.[27] Recently, a nonaqueous chemistry has emerged parallel to the $M_3M'S_4$ chemistry developed in

(20) Binstead, R. A.; Jung, B.; Zuberbühler, A. D. *SPECFIT*; Spectrum Software Associates: Chapel Hill, NC, 2000.

(21) *SAINT*, version 6.2; Bruker Analytical X-ray Systems: Madison, WI, 2001.
(22) Sheldrick, G. M. *SADABS Empirical Absorption Program*; University of Göttingen: Göttingen, Germany, 1996.
(23) Sheldrick, G. M. *SHELXTL*, version 5.1; Bruker Analytical X-ray Systems: Madison, WI, 1997.
(24) Llusar, R.; Uriel, S. *Eur. J. Inorg. Chem.* **2003**, 1271.
(25) Shibahara, T. *Coord. Chem. Rev.* **1993**, *123*, 73.
(26) Hernandez-Molina, R.; Sykes, A. G. *J. Chem. Soc., Dalton Trans.* **1999**, 3137.
(27) Fedin, V. P.; Seo, M. S.; Saysell, D. M.; Dybtsev, D. N.; Elsegood, M. R. J.; Clegg, W.; Sykes, A. G. *Dalton Trans.* **2002**, 138.

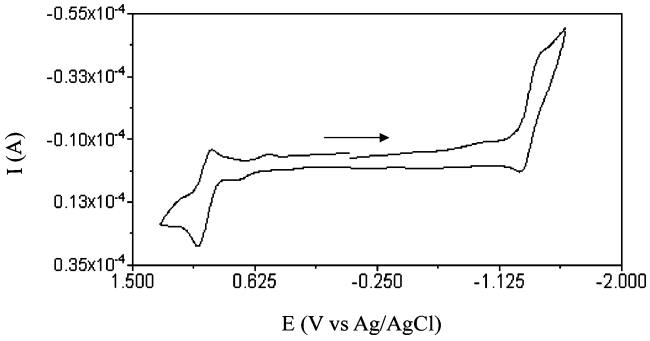

Figure 1. Cyclic voltammogram of $[W_3PdS_4Cl_3(dmpe)_3(CO)][PF_6]$ ($[\mathbf{2}][PF_6]$) registered at 250 mV/s.

water. Typical precursors used are the cyclopentadienyl $[M_3S_4(\eta^5\text{-Cp}')_3]^+$ clusters and the diphosphine $[M_3S_4X_3(\text{diphosphine})_3]^+$ cations. In the case of palladium, the synthesis of $[W_3PdS_4Cp'_3(PPh_3)]^+$ in 92% yield starting from $[W_3S_4(\eta^5\text{-Cp}')_3]^+$ and $[Pd_2(dba)_3]$ in the presence of PPh_3 has been reported.[28] In a similar way, reaction of the trinuclear $[W_3S_4H_3(dmpe)_3]^+$ cation with $[Pd_2(dba)_3]$ followed by CO treatment results in the high-yield formation of the heterodimetallic $[W_3PdS_4H_3(dmpe)_3(CO)]^+$ ($[\mathbf{1}]^+$) cluster hydride. Complex $[\mathbf{1}]^+$ reacts with HCl with substitution of the terminal hydride ligands by chloride to afford $[W_3PdS_4Cl_3(dmpe)_3(CO)]^+$ ($[\mathbf{2}]^+$) in 87% yields. As found for their trinuclear $[W_3S_4H_3(dmpe)_3]^+$ precursor, the reaction is acid-promoted and no ligand replacement is observed with halide salts in the absence of acids. Details on the reaction mechanism of $[\mathbf{1}]^+$ with acids are given in a later section.

The cyclic voltammogram of $[\mathbf{2}]^+$ is represented in Figure 1, with one irreversible reduction wave at -1.31 V and one quasireversible oxidation process at $+1.00$ V. A similar redox behavior has been seen for $[W_3PdS_4(\eta^5\text{-Cp}')_3(PPh_3)]^+$, with a chemically reversible one-electron reduction ($E_{1/2}{}^{+/0} = -1.35$ V) and a two-electron oxidation ($E_{1/2} = 0.52$ V) followed by a first-order reversible chemical reaction. By analogy, we can tentatively identify the two redox waves seen for $[\mathbf{2}]^+$ on the basis of the assignment for $[W_3PdS_4(\eta^5\text{-Cp}')_3(PPh_3)]^+$, although confirmation of this hypothesis is out of the scope of this work.[28] In the case of $[\mathbf{1}]^+$, no reduction wave can be seen because of the closeness of the process to the solvent discharge. It is well-known that trinuclear $[W_3S_4H_3(\text{diphosphine})_3]^+$ hydride complexes are more difficult to reduce than their corresponding halides.[11] On the other hand, $[W_3PdS_4H_3(dmpe)_3(CO)]^+$ ($[\mathbf{1}]^+$) is easier to oxidize than $[\mathbf{2}]^+$, with a half potential value $E_{1/2} = 0.53$ V, similar to that measured for $[W_3PdS_4(\eta^5\text{-Cp}')_3(PPh_3)]^+$. For the oxidation wave in $[\mathbf{1}]^+$ and $[\mathbf{2}]^+$, we observed a decrease in the $i_{p,c}/i_{p,a}$ ratio with the scan rate, in agreement with a chemical process following the electron removal.

The insertion of the $Pd(PPh_3)$ fragment into the $[W_3S_4(\eta^5\text{-Cp}')_3]^+$ cluster produces a cathodic shift of 230 mV in the reduction potential and an anodic shift of ca. 1 V in the potential of the oxidation wave. In our system, the same tendency is observed, although the shifts upon Pd(CO)

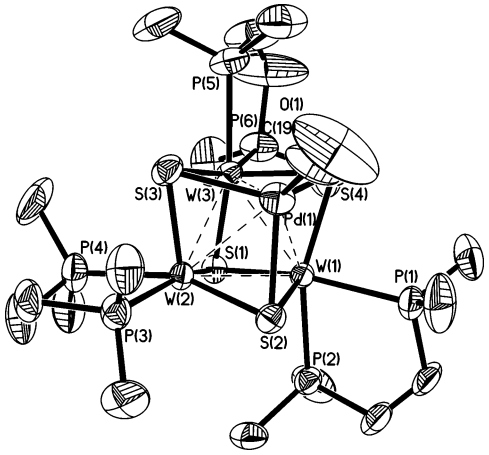

Figure 2. ORTEP representation of the cationic cluster $[W_3PdS_4H_3(dmpe)_3(CO)]^+$ ($[\mathbf{1}]^+$).

incorporation cannot be quantified, because neither the reduction wave for $[\mathbf{1}]^+$ nor the oxidation process for $[W_3S_4H_3(dmpe)_3]^+$ is observed within the solvent window. As a consequence, coordination of the palladium fragment to the cuboidal W_3S_4 cluster unit exerts an electron-donating effect. At this point, it is interesting to analyze how this effect influences the reactivity of the hydride ligands coordinated to the tungsten atoms in these W_3PdS_4 clusters. Although one may expect a higher basicity of the hydride ligands upon Pd incorporation, the opposite effect is observed (vide infra), so the additional electron density is not localized in the W−H bond.

Structure. Compound $[\mathbf{1}][BPh_4]$ crystallizes in the monoclinic $C2/c$ space group without a crystallographically imposed C_3 symmetry; however, the small differences in the intermetallic W−W distances are indicative of an effective C_3 symmetry, in agreement with the presence of two different resonance signals in the $^{31}P\{^1H\}$ NMR spectra. Figure 2 shows an ORTEP drawing of the $[\mathbf{1}]^+$ cluster cation, together with the atom-numbering scheme. The metal cluster core consists of a slightly distorted tetrahedral arrangement of one palladium and three tungsten atoms. Each tetrahedral face is capped by a μ_3-coordinated sulfide ligand, thus generating a cubane-like structure. The coordination sphere on each tungsten atom is essentially octahedral, whereas the palladium atom appears in a tetrahedral environment. For the metal site W(1) (also applicable to W(2) and W(3)), there are two phosphorus atoms, P(1) and P(2), located trans to μ_3-S(1) and μ_3-S(4), respectively, and a vacant position associated with the hydride ligand trans to the μ_3-S(2) bridging ligand. The existence of three hydride ligands, one on each W atom, has been fully supported by ^1H and ^{31}P NMR spectroscopy. The ^1H spectra in the hydride region show a doublet of doublets centered at -2.68 ppm, consistent with three equivalent hydrides coupled with the two nonequivalent phosphorus atoms bonded to the same metal with $^2J_{PH} = 46.0$ and 28.5 Hz. The ^{31}P NMR spectrum registered when selective decoupling of all but the hydridic hydrogen nuclei shows a splitting of the signals with $^2J_{PH}$ coupling constants of 45.4 and 27.3 Hz. These values agree within the experimental error with those measured from the ^1H

(28) Herbst, K.; Zanello, P.; Corsini, M.; D'Amelio, N.; Dahlenburg, L.; Brorson, M. *Inorg. Chem.* **2003**, *42*, 974.

Table 1. Selected Average Bond Distances (Å) for Compounds $[W_3PdS_4H_3(dmpe)_3(CO)][BPh_4]$ ([**1**][BPh_4]), $[W_3S_4H_3(dmpe)_3][BPh_4]$, and $[W_3PdS_4Cp'_3(PPh_3)][Pts]$[a]

bond	[**1**][BPh_4]	$[W_3S_4H_3(dmpe)_3]$-[BPh_4][10]	$[W_3PdS_4Cp'(PPh_3)]$-[pts][28]
W−W	2.769[10]	2.751[4]	2.805[8]
W−Pd	2.90[2]		2.910[9]
Pd−(μ_3-S)	2.472[9]		2.403[5]
W−(μ_3-S)	2.370[6]	2.335[9]	2.326[6]

[a] Standard deviations for averaged values are given in brackets.

spectrum, confirming the presence of one hydrogen atom attached to each metal site.

The tetrahedral environment on the palladium Pd(1) is defined by three bridging sulfur atoms and one carbonyl neutral fragment. Table 1 shows the most-relevant bond distances within the cluster unit in [**1**][BPh_4] together with those found for its trinuclear precursor $[W_3S_4H_3(dmpe)_3]$-[BPh_4].

The average W−W and W−Pd bond distances of 2.769[10] and 2.90[2] Å, respectively, are consistent with the presence of single bonds between metal atoms. There are no significant changes on the W−W bond lengths on going from $[W_3S_4H_3(dmpe)_3]^+$ to $[W_3PdS_4H_3(dmpe)_3(CO)]^+$, whereas the W−S bond distance is elongated by 0.04 Å upon incorporation of the Pd(CO) fragment with a Pd−S distance of 2.472[9] Å. This complex shares structural features with the other structurally characterized W_3Pd cluster, namely $[W_3PdS_4(\eta^5\text{-}Cp')_3(PPh_3)]^+$, although in this case, the W−S bond lengths are considerably shorter, specifically 0.05 and 0.07 Å shorter for the W−S and Pd−S distances, respectively.[28] To visualize these differences, it is illustrative to look at the cuboidal W_3PdS_4 arrangement as two interpenetrated tetrahedrons, one formed by the W_3Pd unit and the other by the four capping sulfur atoms. Elongation of the W−S and Pd−S bond distances implies an expansion of the sulfur tetrahedron, also reflected by the opening of the S−W−S and S−Pd−S angles in the [**1**][BPh_4] cluster complex.

The CO ligand in $[\mathbf{1}]^+$ is coordinated to the Pd atom in an essentially linear Pd−C−O linkage with an angle of 174.8(16)°. The short Pd−C bond length of 1.926 (13) Å indicates a substantial π-back-donation from the Pd center to the CO ligand, also reflected in the low values of 2008 cm^{-1} measured for ν(CO) infrared stretching frequencies. Although this ν(CO) frequency is higher than in known Pd(0) complexes, it is also significantly lower than in Pd^{2+} complexes.[29,30] Theoretical calculations suggest that the high CO stretching frequencies are not a consequence of the heterometal oxidation but rather are the result of the dual role of the heterometal d orbitals, which participate in the formation of the W−Pd bond and in back-bonding to the CO ligand.[31] Although oxidation state assignment in cubane type transition-metal complexes is a polemic task because of the strong electron delocalization, there is no question on the basis of the electrochemical results regarding the electron-donor character of the Pd(CO) fragment upon coordination to the W_3S_4 unit.

In cluster $[\mathbf{1}]^+$, the extra electron density due to the heterometal incorporation results in the formation of three W−Pd bonds and three Pd−S bonds, in which the metal and sulfur orbitals participate in the formation of cluster orbitals delocalized over the entire W_3PdS_4 framework. The electron-donating capability of the Pd(CO) fragment is also reflected in the lengthening of the W−S bonds and expansion of the sulfur tetrahedron. However, this extra electron density surprisingly causes a decrease in the basicity of the hydride ligands coordinated to the tungsten atom; therefore, insertion of the heterometallic fragment to the W_3S_4 complex results in a redistribution of the electron density within the cluster core and the resulting effect on the W−H bond is a net withdrawal of electron density with regard to its trinuclear precursor. Thus, such diminution in the W−H electron density causes a decrease in the basicity of the coordinated hydrides, as will be seen in the next section.

Kinetics of the Reaction of Cluster $[\mathbf{1}]^+$ with Acids. The heterodimetallic cluster $[W_3PdS_4H_3(dmpe)_3(CO)]^+$ ($[\mathbf{1}]^+$) reacts with acids (HCl) to form $[W_3PdS_4Cl_3(dmpe)_3(CO)]^+$ ($[\mathbf{2}]^+$) in a way similar to that for the trinuclear $[W_3Q_4H_3(dmpe)_3]^+$ (Q = S, Se) cluster hydrides, whereas no reaction occurs when halide salts are used.[16,17] To analyze the influence of the heterometal on the acid-assisted substitution process represented in eq 1, we investigated its kinetics in the presence of coordinating solvents.

$$[W_3PdS_4H_3(dmpe)_3(CO)]^+ + 3HCl \rightarrow [W_3PdS_4Cl_3(dmpe)_3(CO)]^+ + 3H_2 \quad (1)$$

The kinetics of the reaction in eq 1 was studied in 0.1 mol dm^{-3} Et_4NBF_4 under pseudo-first-order conditions of acid excess in water−acetonitrile mixtures (1:1 v/v); kinetic features quite similar to those previously reported for the related complexes with incomplete cuboidal structure were observed.[17,18] A typical example of the spectral changes with time for the reaction in eq 1 is shown in Figure 3, where the inset plot is a representative kinetic trace extracted at 442.9 nm. These experimental data were satisfactorily fitted by using a model with three consecutive exponentials (eq 2), which yields the values of the rate constants for the three steps (k_{1obs}, k_{2obs}, and k_{3obs}) and the spectra of the starting complex, the reaction intermediates $\mathbf{I}_1$ and $\mathbf{I}_2$, and the final reaction product (Figure 4). The first-order dependence with respect to $[\mathbf{1}]^+$ was confirmed for all the steps by the lack of changes in the three observed rate constants when the complex concentration was changed.

$$[W_3PdS_4H_3(dmpe)_3(CO)]^+ + 3HCl \xrightarrow[k_{1obs}]{} \mathbf{I}_1 \xrightarrow[k_{2obs}]{} \mathbf{I}_2 \xrightarrow[k_{3obs}]{} [W_3PdS_4Cl_3(dmpe)_3(CO)]^+ + 3H_2 \quad (2)$$

The rate constants for the first step (k_{1obs}) change with the acid concentration according to eq 3 (see Figure 5), and the value derived for the corresponding second-order rate constant is $k_1 = 7.7 \pm 0.1$ dm^3 mol^{-1} s^{-1}. In contrast, the

(29) Yu, L.; Srinivas, G. N.; Schwartz, M. *J. Mol. Struct. (THEOCHEM)* **2003**, *625*, 215.
(30) Vicente, J.; Arcas, A.; Borrachero, M. V.; Tiripicchio, A.; Camellini, M. T. *Organometallics* **1991**, *10*, 3873.
(31) Bahn, C. S.; Tan, A.; Harris, S. *Inorg. Chem.* **1998**, *37*, 2770.

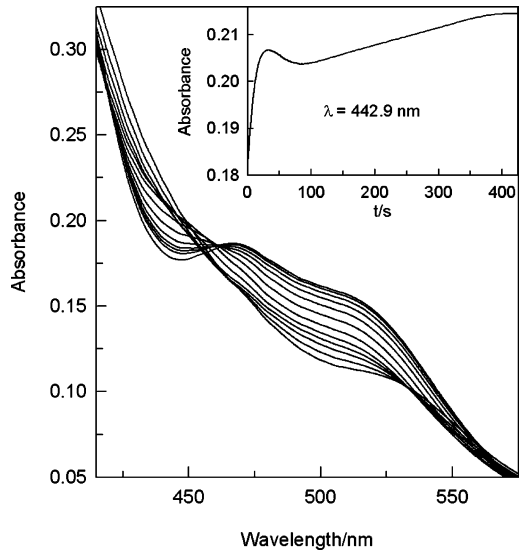

Figure 3. Typical spectral changes with time for the reaction of [**1**][PF_6] with HCl in CH_3CN-H_2O (1:1 v/v) at 25.0 °C. The inset represents the extracted kinetic trace at 442.9 nm.

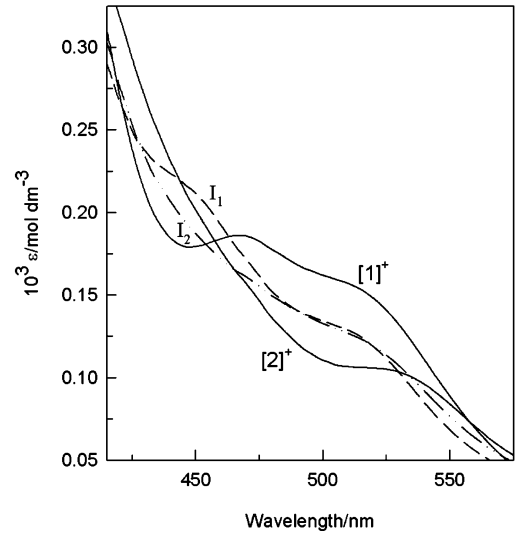

Figure 4. UV−vis spectra calculated for the starting complex [**1**]$^+$, the reaction intermediates (**I**$_1$) and (**I**$_2$), and the final reaction product [**2**]$^+$ for the reaction of [**1**]$^+$ with HCl in $CH_3CN-H2O$ (1:1 v/v).

rate constants for the last two steps (k_{2obs} and k_{3obs}) are independent of the concentration of acid: $k_2 = (5.6 \pm 0.6) \times 10^{-2}$ s^{-1} and $k_3 = (1.0 \pm 0.2) \times 10^{-2}$ s^{-1}.

$$k_{1obs} = k_1[H^+] \quad (3)$$

To obtain more information about the effect of the Pd heterometal on the mechanism of the acid-assisted substitution in this kind of hydride clusters, we also attempted kinetic studies in neat CH_3CN. Surprisingly, no reaction between [**1**]$^+$ and HCl occurs in this solvent, even when the acid concentration is quite high (up to ca. 0.5 mol dm^{-3}). Because the corresponding trinuclear cluster $[W_3S_4H_3(dmpe)_3]^+$ reacts with lower concentrations of HCl in similar conditions, it must be concluded that the presence of the Pd(CO) unit changes the thermodynamics of the process. The decrease in the basicity of the coordinated hydrides in [**1**]$^+$ indicates that despite the electron-donating capability of the Pd(CO) fragment to the W_3S_4 core, the W−H electron density in [**1**]$^+$ is lower than in the trinuclear cluster precursor, $[W_3S_4H_3(dmpe)_3]^+$.

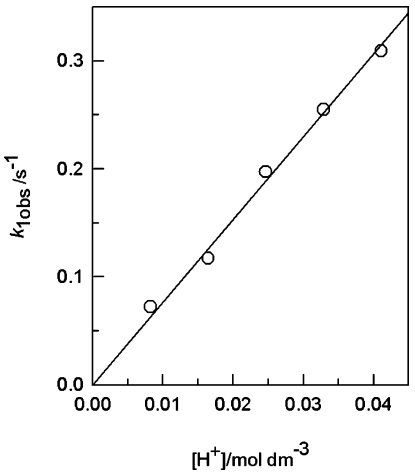

Figure 5. Plot of the observed rate constant for the first step in the reaction of [**1**]$^+$ with HCl in CH_3CN-H_2O (1:1 v/v) mixtures (25.0 °C, 0.1 mol dm^{-3} Et_4NBF_4). The solid line corresponds to the overall fit of each set of data.

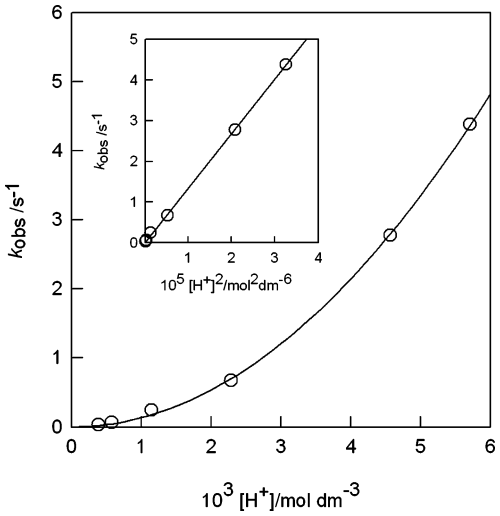

Figure 6. Plot of the observed rate constant for the reaction of [**1**]$^+$ with HBF_4 in neat CH_3CN at 25.0 °C (0.1 mol dm^{-3} Et_4NBF_4).

Because no reaction was observed in acetonitrile solution using [**1**][PF_6] and HCl, the stronger acid HBF_4 was used to obtain information about the kinetics of proton transfer in this solvent, and significant spectral changes were then observed. The kinetic study revealed that the reaction of [**1**]$^+$ with HBF_4 in CH_3CN (0.10 mol dm^{-3} Et_4NBF_4) occurs in a single step, with observed rate constants k_{obs} that show a second-order dependence on the concentration of acid (eq 4, Figure 6) with a value of $k_{HBF4} = (1.34 \pm 0.01) \times 10^5$ dm^6 mol^{-2} s^{-1}. Interestingly, the final UV−vis spectrum observed for the reaction with HBF_4 matches that of intermediate **I**$_1$ obtained by reacting [**1**]$^+$ with HCl. As BF_4^- coordination appears unlikely and the spectrum of this species is independent of both the nature of the acid and the presence of H_2O in the solvent, the most likely formulation for **I**$_1$ is $[W_3PdS_4(CH_3CN)_3(dmpe)_3(CO)]^{4+}$. Unfortunately, attempts to study the kinetics of the reaction with HBF_4 in CH_3CN-H_2O (1:1) mixtures yield complex spectral changes that

suggest the existence of fluoride-abstraction processes, as previously observed for $[W_3S_4H_3(dmpe)_3]^+$.[17] To avoid that problem, HBF_4 was substituted by Hpts, and the supporting electrolyte was changed to Lipts. The reaction of $[\mathbf{1}]^+$ with an excess of Hpts occurs with spectral changes that can be fitted by a single exponential both in neat CH_3CN and CH_3CN-H_2O (1:1) mixtures. The spectrum of the reaction product in both solvents is identical and matches within experimental error with that found for the reaction product with HBF_4 supporting the formulation of $\mathbf{I}_1$ as $[W_3PdS_4(CH_3CN)_3(dmpe)_3(CO)]^{4+}$. The values of the observed rate constants with Hpts in both solvents show a first-order dependence with respect to the acid (see the Supporting Information), with second-order rate constants of $(3.4 \pm 0.1) \times 10^3$ dm^3mol^{-1} s^{-1} in neat CH_3CN and 6.6 ± 0.1 dm^3mol^{-1} s^{-1} in CH_3CN-H_2O mixtures. The latter value compares well with that derived for the first step in the reaction with HCl, confirming that this step is kinetically controlled by proton attack on the cluster. In contrast, in neat CH_3CN, both the rate constant and the rate law change when the acid is changed from HBF_4 to Hpts, which adds further support to previous proposals stating that (H^+, X^-) ion pairs play an active role in the protonation of metal hydrides in aprotic solvents.[32,33]

$$k_{obs} = k_{HBF4}[H^+]^2 \quad (4)$$

To confirm the formulation of the reaction product between $[\mathbf{1}]^+$ and HBF_4 in CH_3CN ($\mathbf{I}_1$) as $[W_3PdS_4(CH_3CN)_3(dmpe)_3(CO)]^{4+}$, we monitored the process using multinuclear ^1H and $^{31}P\{^1H\}$ NMR and ESI-MS techniques. For this purpose, different aliquots of a solution of HBF_4 were added to a solution of $[\mathbf{1}][PF_6]$, and the NMR spectra were recorded after each addition. Through the adequate selection of the amount of acid added, it is possible to detect the NMR signals of the intermediates formed between the starting reagent and the final product. These NMR experiments showed the sequential formation of two intermediates containing two and one W−H bonds and a final product that does not contain any of these bonds. The signals for the hydride and phosphorus atoms of the intermediate with two W−H bonds appear at $\delta_H = -1.62$ ($^2J_{H,P} = 46.2$ and 28.2 Hz) and −1.98 ($^2J_{H,P} = 49.4$ and 28.6 Hz), and $\delta_P = 2.86$, 0.91, −1.89, −2.84, −6.28, and −13.71. The signals for the intermediate with one W−H bond appear at $\delta_H = -1.61$ ($^2J_{H,P} = 51.9$ and 27.8 Hz) and $\delta_P = 3.50$, 1.33, −0.50, −2.69, −5.41, and −8.49, whereas for the final product, $\delta_P = 1.47$ and 0.17 and there are no hydride signals. The phosphorus spectra of both intermediates show six signals, because reaction at only one or two W−H bonds makes the dmpe ligands at different metal centers nonequivalent. Nevertheless, the symmetry is recovered when reaction occurs at the third metal center, so only two signals are observed again. These NMR results indicate that the single step observed in the kinetic experiments actually corresponds to a process that occurs sequentially at the three metal centers with statistically controlled kinetics. In that case, the experimental kinetic traces yield only the observed rate constant for the reaction at the third metal center, although the rate constants for reaction at the three metal centers can be easily derived because they are in a 3:2:1 ratio.[18] It is interesting to note that the kinetics of the reaction of the incomplete cluster $[W_3S_4H_3(dmpe)_3]^+$ with acids was also found to be statistically controlled in neat CH_3CN and CH_3CN-H_2O mixtures,[17] although significant deviations from the statistical predictions were observed in CH_2Cl_2 solution.[18]

Attempts to prepare and isolate the hypothetical species $[W_3PdS_4(CH_3CN)_3(dmpe)_3(CO)]^{4+}$ were carried out by reacting the hydride cluster $[\mathbf{1}]^+$ in acetonitrile with an excess of aqueous HBF_4. After precipitation with diethyl ether, a brown solid was obtained. Multinuclear NMR spectra of this solid dissolved in acetone-d_6 share common features with those recorded for the $[\mathbf{1}][PF_6]$ and $[\mathbf{2}][PF_6]$ clusters. In particular, two phosphorus signals are observed in the $^{31}P\{^1H\}$ spectra, and the characteristic four doublets pattern (due to the four methyl groups of each diphosphine) is observed in the ^1H spectra. Additionally, the ^1H spectra reveal the presence of one singlet at 1.9 ppm with an intensity similar to that of the methyl groups; the singlet is assigned to the coordinated acetonitrile. ^1H-^3C gHSQC experiments further confirm the presence of coordinated acetonitrile (coordinated CH_3CN signal at 12 ppm). This spectrum is given as Supporting Information, together with the spectra of $[\mathbf{1}][PF_6]$ and $[\mathbf{2}][PF_6]$, for comparative purposes. Although NMR spectroscopy provides enough evidence of the presence of $[W_3PdS_4(CH_3CN)_3(dmpe)_3(CO)]^{4+}$ in solution, it has to be pointed out that this species decomposes in acetone, acetonitrile, or dichloromethane solutions in a period of approximately 2 h. All attempts aimed to either obtain this species in analytically pure form or grow single crystals were unsuccessful.

Further support regarding the coordination of CH_3CN into the hydride sites of $[\mathbf{1}]^+$ in acidic media, i.e., HBF_4, has been extracted though an ESI-MS analysis of $[\mathbf{1}][PF_6]$ solutions in CH_3CN at different acid concentrations.The mass spectra clearly showed the presence of coordinated CH_3CN for the first reaction intermediate with a signal centered at 653 amu that is assigned to the $[W_3PdS_4H_2(CH_3CN)(dmpe)_3(CO)]^{2+}$ dication. This signal coexists with another one centered at 633 that can be assigned to the product resulting from the CH_3CN dissociation, namely $[W_3PdS_4H_2(dmpe)_3(CO)]^{2+}$ with a vacant coordination site (see Figure 7). On the basis of the NMR results, which indicate the existence of a single species with two coordinated hydrides, the most likely explanation is to assume that CH_3CN dissociation occurs during the mass spectra recording, although the existence of some degree of dissociation in the reaction mixture cannot be definitely ruled out.

The mass spectra recorded at higher HBF_4 concentrations show a signal centered at 449 that can be assigned to the intermediate with two coordinated acetonitrile molecules of formula $[W_3PdS_4H(CH_3CN)_2(dmpe)_3(CO)]^{3+}$. Unfortunately,

(32) Basallote, M. G.; Duran, J.; Fernandez-Trujillo, M. J.; Manez, M. A.; Rodriguez de la Torre, J. *J. Chem. Soc., Dalton Trans.* **1998**, 745.
(33) Basallote, M. G.; Duran, J.; Fernandez-Trujillo, M. J.; Manez, M. A. *Inorg. Chem.* **1999**, *38*, 5067.

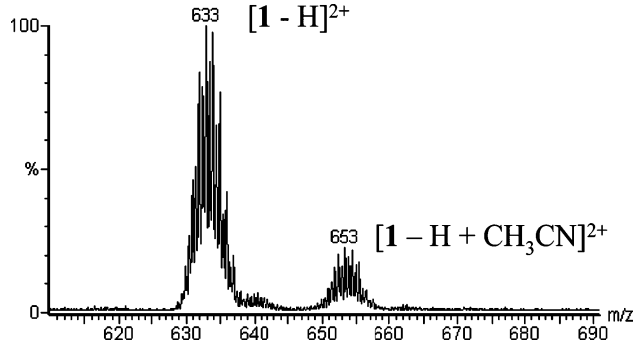

Figure 7. ESI-MS spectra recorded after the addition of 1 equiv of HBF_4 to a solution of compound $[W_3PdS_4H_3(dmpe)_3(CO)][BPh_4]$ ($[\mathbf{1}][BPh_4]$) in acetonitrile.

the MS experiments did not allow for the detection of the final $[W_3PdS_4(CH_3CN)_3(dmpe)_3(CO)]^{4+}$ product because of the high charge of the cluster.

Mechanism of the Reaction of $[1]^+$ with Acids. The experimental information available for the reaction in eq 1 in CH_3CN and CH_3CN−water solution indicates that its mechanism must be rather similar to that proposed for the homometallic cluster precursor $[W_3S_4H_3(dmpe)_3]^+$, which has an incomplete cuboidal structure that lacks the Pd(CO) unit. For the reaction of the incomplete cluster, the acid-promoted substitution of the coordinated hydrides by Cl^- was explained in terms of the mechanism in eqs 5−8,[17] in which the initial attack by the acid to the W−H bond yields an unstable dihydrogen complex (eq 5) that rapidly releases H_2 and forms a coordinatively unsaturated complex (eq 6). This complex adds water in the next step (eq 7); finally, the coordinated water is substituted by the Cl^- anion (eq 8). Although, for simplicity, eqs 5−8 have been written showing the reaction at a single metal center, all these processes actually occur sequentially at each one of the three W−H bonds with statistically controlled kinetics.

$$[W_3S_4H_3(dmpe)_3]^+ + HCl \xrightarrow[k_{1obs}]{} [W_3S_4H_2(H_2)(dmpe)_3]^{2+} + Cl^- \quad (5)$$

$$[W_3S_4H_2(H_2)(dmpe)_3]^{2+} \xrightarrow[\text{fast}]{} [W_3S_4H_2(dmpe)_3]^{2+} + H_2 \quad (6)$$

$$[W_3S_4H_2(dmpe)_3]^{2+} + solv \xrightarrow[k_{2obs}]{} [W_3S_4H_2(solv)(dmpe)_3]^{2+} \quad (7)$$

$$[W_3S_4H_2(solv)(dmpe)_3]^{2+} + X^- \xrightarrow[k_{3obs}]{} [W_3S_4H_2X(dmpe)_3]^+ \quad (8)$$

However, recent theoretical calculations have revealed that the formation of solvent adducts such as $[W_3PdS_4(CH_3CN)_3(dmpe)_3(CO)]^{4+}$ ($\mathbf{I}_1$) is favored in front of dihydrogen complexes and/or coordinatively unsaturated species (eqs 5 and 6) and that proton attack on trinuclear cluster hydrides occurs through the diffusion-controlled initial formation of W−H···HCl dihydrogen-bonded adducts.[18] Acetonitrile attack on the W−H···HCl dihydrogen-bonded species produces the $\mathbf{I}_1$ intermediate. The observation of intermediate $\mathbf{I}_1$ from the reactions of cluster $[\mathbf{1}]^+$ with HBF_4 and Hpts in CH_3CN also supports this interpretation. In this context, the absence of a reaction between $[\mathbf{1}]^+$ and HCl in neat CH_3CN is quite surprising. This can be explained by taking into account the nature of the protonating species; for the reaction with HCl in neat CH_3CN, the protonating species would be the HCl molecule itself, whereas for the other reactions, this is H^+_{solv}. Apparently, the energy cost associated with the rupture of the H−Cl bond makes the reaction in pure CH_3CN unfavorable for cluster $[\mathbf{1}]^+$, in contrast with the hydride substitution observed for $[W_3S_4H_3(dmpe)_3]^+$ under analogous conditions.

Once the nature of $\mathbf{I}_1$ has been established as the cluster resulting from a formal substitution of the hydride ligands by acetonitrile molecules, namely $[W_3PdS_4(CH_3CN)_3(dmpe)_3(CO)]^{4+}$, the unknown factor that remains for a satisfactory mechanistic interpretation of the acid-assisted substitution of the coordinated hydrides in $[\mathbf{1}]^+$ is the determination of the nature of the intermediate $\mathbf{I}_2$, which should be a cluster species halfway between complexes containing W−$NCCH_3$ and W−Cl bonds**.** In the case of the incomplete cluster $[W_3S_4H_3(dmpe)_3]^+$, the preparation of the trihydroxo complex $[W_3S_4(OH)_3(dmpe)_3]^+$ allowed for kinetic and NMR experiments that led to the formulation of $\mathbf{I}_2$ as $[W_3S_4(H_2O)_3(dmpe)_3]^{4+}$.[17] However, in the present case, the observation of a single step in the reaction of $[\mathbf{1}]^+$ with Hpts in a CH_3CN-H_2O mixtures introduces a serious argument against the formulation of $\mathbf{I}_2$ as an aqua complex because, under those conditions, the reaction stops at the $[W_3PdS_4(CH_3CN)_3(dmpe)_3(CO)]^{4+}$ complex despite the large water excess. Given the fact that absorbance changes associated with the conversion of $\mathbf{I}_1$ to $\mathbf{I}_2$ are small and limited to a short wavelength range, we consider the interpretation that these absorbance changes correspond to some unknown secondary process and that the acid-promoted substitution of the coordinated hydrides in $[\mathbf{1}]^+$ actually occurs in two kinetic steps to be a more-plausible interpretation. The first step is represented by eq 9, and the second one would consist of the substitution of CH_3CN by Cl^- with rate constants given by k_{3obs} (eq 10).

$$[W_3PdS_4H_3(dmpe)_3(CO)]^+ + HX \rightarrow [W_3PdS_4H_2(CH_3CN)(dmpe)_3(CO)]^{2+} + H_2 + X^-;\ k_{1obs} \quad (9)$$

$$[W_3PdS_4H_2(CH_3CN)(dmpe)_3(CO)]^{2+} + X^- \rightarrow [W_3PdS_4H_2X(dmpe)_3(CO)]^+ + CH_3CN;\ k_{3obs} \quad (10)$$

The kinetic results obtained for the initial protonation of the coordinated hydrides in cluster $[\mathbf{1}]^+$ deserve some additional comment. There is recent evidence on the existence of competitive first- and second-order pathways for the protonation of the coordinated hydrides in $[W_3S_4H_3(dmpe)_3]^+$.[18] The second-order pathway requires two molecules of acid that assist the proton transfer by forming a M−H···H−X···H−X adduct with a shorter H···H distance, which facilitates the subsequent release of H_2. The operation of a second-order mechanism for the proton transfer in other transition-metal hydrides has been associated with the stabilization that results from the formation of homoconjugated HX_2^- species that require the presence of a second

acid molecule.[34,35] As HBF_4 does not exist in molecular form, the kinetics results found in the present work for the reaction of $[\mathbf{1}]^+$ with HBF_4 in CH_3CN (eq 4) demonstrate that operation of the second-order pathway does not require a molecular acid able to form homoconjugated species or a solvent with a low dielectric constant, which indicates that the formation of the homoconjugated HX_2^- species does not play a substantial role in the protonation of these clusters. In the case of these W_3S_4 or W_3PdS_4 cluster hydrides, the role of the second equivalent of acid in the second-order pathway seems to be mainly related to the formation of a network of hydrogen bonds that prepare the system for H_2 release.[18] We are currently carrying out both theoretical calculations and kinetic work on the reaction of $[\mathbf{1}]^+$ with acids in dichloromethane solution in an attempt to gain new insights into the effects caused by the introduction of the Pd(CO) subunit into the different mechanistic pathways for the proton transfer to the coordinated hydrides.

As a summary, the results in the present work demonstrate that incorporation of Pd into the $[W_3S_4H_3(dmpe)_3]^+$ cluster produces air-stable heterodimetallic cubane type hydrido clusters in high yields. Whereas the W−H bonds in these W_3PdS_4 complexes show a reactivity similar to that found for the trinuclear hydride precursor, insertion of the heterometal modulates both the thermodynamics and the kinetics of the proton-transfer reaction at the W−H centers. In particular, there is an unexpected basicity decrease in the hydride ligands despite the electron-donating character found for the Pd(CO) fragment, which suggests an extensive reorganization of the electron density upon heterometal insertion that is also reflected in a significant expansion of the sulfur tetrahedron within the W_3PdS_4 core. However, for those thermodynamically favored processes, the kinetic data available indicate that the reaction mechanism is quite similar to that observed for the incomplete trinuclear cluster, with only small variations in the rate constants.

Acknowledgment. The financial support of the Spanish Ministerio de Educación y Ciencia and the EU FEDER Program (Grants CTQ2005-09270-C02-01and BQU2003-04737), Fundació Bancaixa-UJI (Project P1.1B2004-19), Junta de Andalucía (Grupo FQM-137), and Generalitat Valenciana (Project ACOMP06/241) is gratefully acknowledged. The authors also thank the Servei Central D'Instrumentació Cientifica (SCIC) of the Universitat Jaume I and the Servicios Centrales de Ciencia y Tecnología of the Universidad de Cádiz for providing us with the mass spectrometry, NMR, and X-ray facilities.

Supporting Information Available: X-ray crystallographic information in CIF format; plots of the dependence of the observed rate constant with the concentration of Hpts in acetonitrile (Figure S1) and acetonitrile−water (Figure S2) solution; and $^1H-^{13}C$ gHSQC spectra for compounds $[\mathbf{1}][PF_6]$ (Figure S3), $[\mathbf{2}][PF_6]$ (Figure S4), and species $[W_3PdS_4(CH_3CN)_3(dmpe)_3(CO)][PF_6]_x[BF_4]_{x-4}$ (Figure S5). This material is available free of charge via the Internet at http://pubs.acs.org.

IC052184U

(34) Papish, E. T.; Rix, F. C.; Spetseris, N.; Norton, J. A.; Williams, R. D. *J. Am. Chem. Soc.* **2000**, *122*, 12235.
(35) Belkova, N. V.; Besora, M.; Epstein, L. M.; Lledós, A.; Maseras, F.; Shubina, E. S. *J. Am. Chem. Soc.* **2003**, *125*, 7715.